

Hybrid Kriging-assisted Level Set Method for Structural Topology Optimization

Elena Raponi¹^a, Mariusz Bujny^{2,3}^b, Markus Olhofer²^c, Simonetta Boria¹^d
and Fabian Duddeck^{3,4}^e

¹*School of Sciences and Technologies, Department of Mathematics, University of Camerino, Camerino, Italy*

²*Honda Research Institute Europe GmbH, Offenbach am Main, Germany*

³*Department of Civil, Geo and Environmental Engineering, Technical University of Munich, Munich, Germany*

⁴*School of Engineering and Materials Science, Queen Mary University of London, London, U.K.*


Keywords: Topology Optimization, Structural Optimization, Hybrid Methods, Surrogate Modeling, Kriging, Evolution Strategies, Level Set Method, Moving Morphable Components.


Abstract: This work presents a hybrid optimization approach that couples Efficient Global Optimization (EGO) and Covariance Matrix Adaptation Evolution Strategy (CMA-ES) in the Topology Optimization (TO) of mechanical structures. Both of these methods are regarded as good optimization strategies for continuous global optimization of expensive and multimodal problems, e.g. associated with vehicle crashworthiness. CMA-ES is flexible and robust to changing circumstances. Moreover, by taking advantage of a low-dimensional parametrization introduced by the Evolutionary Level Set Method (EA-LSM) for structural Topology Optimization, such Evolution Strategy allows for dealing with costly problems even more efficiently. However, it is characterized by high computational costs, which can be mitigated by using the EGO algorithm at the early stages of the optimization process. By means of surrogate models, EGO allows for the construction of cheap-to-evaluate approximations of the objective functions, leading to an initial fast convergence towards the optimum in opposition to a poor exploitive behavior. The approach presented here – the Hybrid Kriging-assisted Level Set Method (HKG-LSM) – first uses the Kriging-based method for Level Set Topology Optimization (KG-LSM) to converge fast at the beginning of the optimization process and explore the design space to find promising regions. Afterwards, the algorithm switches to the EA-LSM using CMA-ES, whose parameters are initialized based on the previous model. A static benchmark test case is used to assess the proposed methodology in terms of convergence speed. The obtained results show that the HKG-LSM represents a valuable option for speeding up the optimization process in real-world applications with limited computational resources. As such, the proposed methodology exhibits a much more general potential, e.g. when dealing with high-fidelity crash simulations.


1 INTRODUCTION


Over the last decades, vehicle safety has become one of the most studied research areas in automotive engineering. In particular, since physical experiments are characterized by prohibitive times and costs, the design phase of new structures and components need particular attention. The development of Computer-


Aided Design (CAD) methods and the progress in numerical simulations with the Finite Element Method (FEM) have made Crashworthiness Design a discipline of increasing interest and potential. An option to face the concept selection and the generation of a prototype is embodied by Structural Topology Optimization (TO) (Bendsøe and Sigmund, 2004). TO is a well-developed discipline that aims to determine constructive solutions for component structures through changing material distribution in a given design space so as to obtain an optimal concept design under defined boundary conditions (supports, forces). Although it is applied in many engineering fields, the most known TO approaches for crashworthiness ap-

^a <https://orcid.org/0000-0001-6841-7409>

^b <https://orcid.org/0000-0003-4058-3784>

^c <https://orcid.org/0000-0002-3062-3829>

^d <https://orcid.org/0000-0003-2073-4012>

^e <https://orcid.org/0000-0001-8077-5014>

plications might be questioned because they use simplifications, which frequently do not take into account important aspects of the crash problem, e.g. nonlinearities, numerical noise, and discontinuities of the objective functions to be optimized. Such approaches can be collected in the following categories: Equivalent Static Loads method (Duddeck and Volz, 2012; Lee and Park, 2015), Ground Structure Approaches (Pedersen, 2003), Bubble and Graph/Heuristic-based Approaches (Eschenauer et al., 1994; Ortmann and Schumacher, 2013), Hybrid Cellular Automata method (Mozumder et al., 2012; Duddeck et al., 2016), and State-based representation approaches (Aulig and Olhofer, 2016; Aulig, 2017).

In this context, global optimizers which do not require any gradient or sensitivity information to carry out the optimization procedure become of the utmost importance. Among the proposed algorithms for solving crash optimization problems, Evolution Strategies (ES) (e.g., the Covariance Matrix Adaptation Evolution Strategy (CMA-ES) (Hansen and Ostermeier, 1996)) and the Efficient Global Optimization (EGO) (Forrester et al., 2008) demonstrated to be valid alternatives.

On the one hand, ESs handle the update process by directly evaluating the objective function in different points of the design space. Compared to other global optimization techniques, these algorithms are easy to implement and very often provide adequate solutions, showing many advantages such as simplicity, robust responses to changing circumstances and flexibility. However, they require thousands of calls to the high-fidelity analysis codes to locate a near optimal solution, leading to very high numerical costs, which are proportional to the problem dimensionality.

On the other hand, EGO allows for replacing the direct optimization of the computationally expensive model by an iterative process composed of the creation, optimization and update of an approximation of the original function, referred to as Surrogate Model. This model is much cheaper to run and can be used to perform many more evaluations during the optimization process. A limited set of points is initially defined in the problem domain and the real expensive function is here evaluated. Based on the obtained training data, a first approximation of the model is constructed and its accuracy is improved by the algorithm by evaluating new points. Nonetheless, surrogate-based optimization shows some limitation with the increasing of dimensionality and iterations of the algorithm, turning out to have poorer exploitive capabilities than ESs (Raponi et al., 2019).

This research focuses on the development of a Hybrid Surrogate-assisted Modeling Technique

for Structural Topology Optimization, the Hybrid Kriging-assisted Level Set Method (HKG-LSM), which is composed of three major building blocks:

- the Level Set Method (LSM) (Osher and Sethian, 1988; Haber and Bendsøe, 1998; Allaire et al., 2004), which allows for monitoring the material distribution changes according to low-dimensional implicit parametrization of the material boundaries by means of local Level Set Functions (LSFs), also referred to as Movable Morphable Components (MMCs) (Guo et al., 2014);
- the Kriging-guided Level Set Method (KG-LSM) (Raponi et al., 2017; Raponi et al., 2019), which initializes a set of training points to construct a cheap approximating model. By updating the model based on the data points and the committed error in the approximation, it allows for obtaining a trade-off between exploration and exploitation of the domain space, which produces a fast convergence of the algorithm towards promising areas;
- the Evolutionary Level Set Method (EA-LSM) for crash Topology Optimization (Bujny et al., 2016; Bujny et al., 2018), embedding the Covariance Matrix Adaptation Evolution Strategy (CMA-ES), to which the proposed optimization algorithm switches when prescribed conditions are satisfied. Its main role is to investigate the detected good region and further exploit it in order to locally optimize the current design.

In this study, the proposed method is evaluated on a static Cantilever Beam benchmark test case for a fixed budget of FEM evaluations. This choice is dictated by the fact that in many industrial applications, FEM evaluations are very expensive and, as such, limited. Moreover, the static case allows for testing the developed methodology with limited computational effort. The convergence trends, as well as the optimized designs resulting from the considered optimization algorithms, are discussed. Although the validation of the proposed methodology is based on a static test case, the derived results show it could be a valuable tool for identification of optimal concept designs in crashworthiness applications, which cannot be addressed by standard topology optimization methods due to the lack of gradient information.

2 PROBLEM REPRESENTATION

In view of a future application of the HKG-LSM to the Topology Optimization of crash structures, the

method is aimed to easily handle the unpredictability, noisiness, discontinuities and lack of gradient information which characterize the crashworthiness design optimization field. Since in structural mechanics optimal topologies frequently consist of ensembles of interconnected beams, on the basis of previous studies (Guo et al., 2014; Bujny et al., 2018; Raponi et al., 2019), the mechanical structure consists of an ensemble of MMCs, whose boundaries are implicitly defined by iso-contours of a LSF.

2.1 Parametrization

According to the parametrization adopted in previous works (Bujny et al., 2018; Raponi et al., 2019), let the global Level Set Function Φ be defined as:

$$\begin{cases} \Phi(\mathbf{u}) > 0, & \mathbf{u} \in \Omega, \\ \Phi(\mathbf{u}) = 0, & \mathbf{u} \in \partial\Omega, \\ \Phi(\mathbf{u}) < 0, & \mathbf{u} \in D \setminus \Omega, \end{cases} \quad (1)$$

where Ω is the region of the domain D occupied by material, $D \setminus \Omega$ is its complementary set, occupied by void, and $\partial\Omega$ is the interface between material and void. Consequently, intermediate densities are avoided for each $\mathbf{u} = (x, y)^T \in D$.

This global LSF is then composed by local LSFs given by:

$$\begin{cases} \phi_i(\mathbf{u}) > 0, & \mathbf{u} \in \Omega_i, \\ \phi_i(\mathbf{u}) = 0, & \mathbf{u} \in \partial\Omega_i, \\ \phi_i(\mathbf{u}) < 0, & \mathbf{u} \in D \setminus \Omega_i, \end{cases} \quad (2)$$

where ϕ_i is the LSF that parametrizes the i^{th} component, which occupies the design domain region Ω_i .

Therefore, if e is the number of elementary components, the region of the domain occupied by material can be seen as:

$$\Omega = \bigcup_{i=1}^e \Omega_i. \quad (3)$$

Now, let us consider for each beam a local basis function of the form proposed first by Guo et al. (2014):

$$\begin{aligned} \phi_i(\mathbf{u}) = - & \left[\left(\frac{\cos \theta_i (x - x_{0i}) + \sin \theta_i (y - y_{0i})}{l_i/2} \right)^m \right. \\ & \left. + \left(\frac{-\sin \theta_i (x - x_{0i}) + \cos \theta_i (y - y_{0i})}{t_i/2} \right)^m - 1 \right], \end{aligned} \quad (4)$$

where $\mathbf{u} = (x, y)^T$ is a point of the bidimensional domain $D = \mathbb{R}^2$ and (x_0, y_0) denotes the position of the center of the component with length l , thickness t , and oriented inside the domain according to a rotation angle θ , as shown in Figure 1(a). The symbol m stands

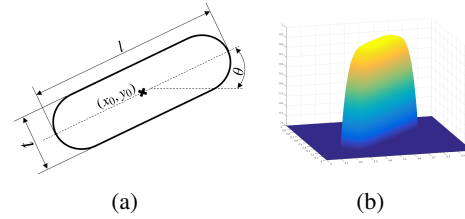


Figure 1: Structural component details (Bujny et al., 2018): (a) Component parametrization, (b) Corresponding local LSF, where negative values are set to zero.

for a relatively large even integer number, taken equal to 6 in this study.

By changing the values of the parameters, each beam can move, dilate or shrink and rotate in the design domain. Figure 1(b) shows a 3-dimensional plot of the i^{th} local LSF corresponding to definition (4).

2.2 Geometry Mapping

In Level Set Topology Optimization it is important to choose a mapping from the geometry defined by the LSF to the mechanical model. Here, due to its simplicity, a density-based geometry mapping is used:

$$\mathbf{E}(\mathbf{u}) = \rho(\mathbf{u}) \mathbf{E}^0 \quad 0 \leq \rho(\mathbf{u}) \leq 1, \quad (5)$$

where $\rho(\mathbf{u})$ is the density at the point $\mathbf{u} \in D$ and \mathbf{E}^0 is the reference value of the stiffness tensor.

Hence, the density $\rho(\mathbf{u})$ at position \mathbf{u} is computed from the LSF $\Phi(\mathbf{u})$ as:

$$\rho(\mathbf{u}) = H(\Phi(\mathbf{u})), \quad (6)$$

where the global LSF is the maximum of the local ones at position \mathbf{u} :

$$\Phi(\mathbf{u}) = \max(\phi_1(\mathbf{u}), \phi_2(\mathbf{u}), \dots, \phi_e(\mathbf{u})), \quad (7)$$

and $H(x)$ is the Heaviside function, which is equal to 0 for negative arguments and equal to 1 for nonnegative ones. Figure 2 shows an example of the composition of local LSFs, resulting in the global LSF given by Equation 7.

3 OPTIMIZATION PROBLEM AND CONSTRAINTS

In this work, an optimization problem of the following form is considered:

$$\begin{aligned} \min_{\mathbf{x}} \quad & f_{\text{obj}}(\mathbf{x}), \\ \text{s.t.} \quad & g_i(\mathbf{x}) \leq 0, \quad i = 1, \dots, m, \quad \mathbf{x} \in \mathbb{R}^k, \end{aligned} \quad (8)$$

where f_{obj} is the objective function that is minimized and g_i , $i = 1, \dots, m$, are the inequality constraints. The

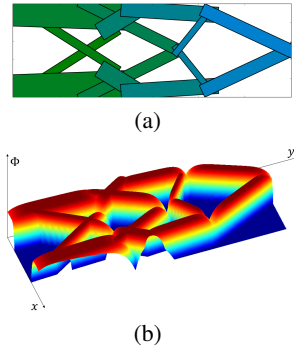


Figure 2: Combination of local Level Set Functions: (a) illustrative structural layout, (b) plot of the global LSF, where negative values are set to zero. (Raponi et al., 2019)

objective function is evaluated on the vector $\mathbf{x} \in \mathbb{R}^k$ of the design variables, which collects all the parameters defining the LSM basis functions. This study minimizes the compliance of a cantilever beam test case in a 9-variables test case. The optimization is carried out while respecting a $g(\mathbf{x}) = V(\mathbf{x}) - V_{\text{req}} \leq 0$ constraint, which requires the volume V of the analyzed structure not to exceed a prescribed limit V_{req} equal to 50% of the design domain volume. Throughout the optimization process, disconnected structures can be obtained, as illustrated in Figure 3. Therefore, in order to be physically consistent, a connectivity constraint is also considered within this work. Such constraint ensures that the optimized structures make sense from the physical point of view, while the volume constraint is imposed in order to make the structures fulfill the industrial requirements of limited mass. Each material distribution has to be connected to the support on the left-hand side of the domain, to the load which the structure is subjected to on the right-hand side, and has to respect a connection of the structure to itself, i.e. a material path from the support to the load has to be found. Figure 3 shows three material distributions, each representing the violation of the connectivity constraint according to the first, second and third criterion, respectively. According to the phase of the optimization procedure, i.e. the sub-algorithm that is currently used, two different techniques are used to handle such constraints, which are described in Section 4.2.

4 RESOLUTION STRATEGY

The following section focuses on the description of the optimization procedure defined within this research. In order to drive the considered structures towards optimum, this work introduces a novel hy-

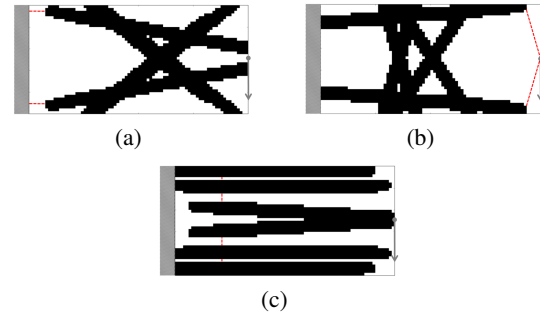


Figure 3: Violation of the connectivity constraint regarding (a) the connection to the support, (b) the connection to the load, (c) the connection of the structure itself. The distances prohibiting the design to fulfill the connectivity criteria are represented by the dashed lines (Raponi et al., 2019).

brid optimization strategy which combines sequentially the EGO with the Kriging model (KG-LSM) and the CMA-ES (incorporated in the EA-LSM). This choice is due to the fact that the EGO is efficient in the early stage of the optimization due to the explorative potential of the infill procedure, while CMA-ES has good exploitative capabilities which makes it to efficiently perform a local search and converge to a final refined structure.

4.1 Optimization Algorithm

The optimization procedure proposed in this work (the HKG-LSM) is tailored to solve efficiently problems in structural mechanics, and applied to the optimization of static Cantilever Beam test cases. It is composed of two sub-algorithms: it first redrafts the EGO algorithm (Jones et al., 1998; Arsenyev, 2017), applied to the Kriging surrogate model, and subsequently it switches to the CMA-ES to finally refine the last structure obtained before the sub-algorithm changes. Algorithm 1 gives an outline of the developed optimization method in case if each constraint is used.

The HKG-LSM algorithm starts with the Design of Experiments (DoE) (Forrester et al., 2008), which samples the design space and selects a set of training points where to evaluate the high-fidelity model. In order to determine a set of training samples, an Optimal Latin Hypercube Sampling (OHLS) (Fang et al., 2005) is used in this work, leading to a training dataset $\mathbf{X} = \{\mathbf{x}^{(1)}, \mathbf{x}^{(2)}, \dots, \mathbf{x}^{(n)}\}^T$ with observed responses $\mathbf{y} = \{y^{(1)}, y^{(2)}, \dots, y^{(n)}\}^T$. For all points, the feasibility according to the volume and connectivity constraints is checked, and based on them a Kriging approximation is fitted and iteratively updated. When the number of iterations where no improvement on the best design is detected reaches an allowed maximum,

Data: initial data set (\mathbf{X}, \mathbf{Y}) with n sample points, where $\mathbf{X} = \{\mathbf{x}^{(1)}, \mathbf{x}^{(2)}, \dots, \mathbf{x}^{(n)}\}^T$

```

i := 1;
while i < n do
  check feasibility of point  $\mathbf{x}^{(i)}$ ;
  if  $\mathbf{x}^{(i)}$  infeasible then
    |  $\mathbf{X} := \mathbf{X} \setminus \{\mathbf{x}^{(i)}\}$ 
  end
  i := i + 1;
end
y* := min( $\mathbf{Y}$ );
 $\mathbf{x}^*$  :=  $\mathbf{x} \in \mathbf{X} : y(\mathbf{x}) = y^*$ ;
t := 0;
c := 1
while t <  $n_{max}$  and c <  $c_{max}$  do
  fit Kriging to available data  $(\mathbf{X}, \mathbf{Y})$ ;
  find infill point:  $\mathbf{p} := \operatorname{argmax}_{\mathbf{x}} \overline{\text{EICD}}(\mathbf{x})$ 
  (Equation (23));
  update sample set:  $\mathbf{X} := \mathbf{X} \cup \mathbf{p}$ ;
  update response set:  $\mathbf{Y} := \mathbf{Y} \cup y(\mathbf{p})$ ;
  if min( $\mathbf{Y}$ ) < y* then
    | c := 1;
    | y* := min( $\mathbf{Y}$ );
    |  $\mathbf{x}^* := \mathbf{x} \in \mathbf{X} : y(\mathbf{x}) = y^*$ ;
  else
    | c := c + 1;
  end
  t := t + 1;
end
initialize CMA-ES parameters  $(\sigma, C)$ ;
initialize parent design:  $\mathbf{x} = \mathbf{x}^*$ ;
run CMA-ES.

```

Algorithm 1: HKG-LSM optimization algorithm. The reference algorithm for the CMA-ES can be found in the work by Hansen (Hansen, 2006).

the optimizer passes from the Kriging-based strategy to the CMA-ES, whose parent design is set as the best structure found by the previous sub-algorithm.

4.1.1 Kriging Model

The Kriging Surrogate Model (Cressie, 1990; Forrester et al., 2008; Kleijnen, 2009; Arsenyev, 2017) aims to predict the value of an unknown function at a given point by computing a weighted average of the already known values of the function in the neighborhood of that point.

Starting from a set of sample data $\mathbf{X} = \{\mathbf{x}^{(1)}, \mathbf{x}^{(2)}, \dots, \mathbf{x}^{(n)}\}^T$ with observed responses $\mathbf{y} = \{y^{(1)}, y^{(2)}, \dots, y^{(n)}\}^T$, the aim is to predict the objective function value at the location \mathbf{x} .

Let the training data be seen as results of a stochastic process, which is described with use

of a set of random vectors of the form $\mathbf{Y}(\mathbf{x}) = (Y(\mathbf{x}^{(1)}), \dots, Y(\mathbf{x}^{(n)}))^T$, with mean $\mathbf{1}\mu$, where $\mathbf{1}$ is an $n \times 1$ column vector of ones. Moreover, let the correlation between each couple of random variables be described using a basis function expression:

$$\operatorname{cor}[Y(\mathbf{x}^{(i)}), Y(\mathbf{x}^{(l)})] = \exp\left(-\sum_{j=1}^k \theta_j |x_j^{(i)} - x_j^{(l)}|^2\right). \quad (9)$$

where the θ vector allows the width of the basis function to differ from variable to variable. The correlations depend on the absolute distance between the sample points and on the parameters θ_j , which are estimated by using the likelihood of the predicted data \mathbf{y} (Forrester et al., 2008):

$$L = \frac{1}{(2\pi\sigma^2)^{n/2} |\Psi|^{1/2}} \exp\left(-\frac{(\mathbf{y} - \mathbf{1}\mu)^T \Psi^{-1} (\mathbf{y} - \mathbf{1}\mu)}{2\sigma^2}\right). \quad (10)$$

After appropriate substitutions and simplifications, the natural logarithm of Equation (10) is considered. By deriving and setting the derivative to zero, the maximum likelihood estimates (MLEs) for the mean μ and variance σ^2 are obtained:

$$\hat{\mu} = \frac{\mathbf{1}^T \Psi^{-1} \mathbf{y}}{\mathbf{1}^T \Psi^{-1} \mathbf{1}}, \quad \hat{\sigma}^2 = \frac{(\mathbf{y} - \mathbf{1}\mu)^T \Psi^{-1} (\mathbf{y} - \mathbf{1}\mu)}{n}, \quad (11)$$

where Ψ is the correlation matrix between the random variables. Finally, the model correlation can be utilized to predict new values based on the observed data. By augmenting the model data with a new input \mathbf{x} and the corresponding output \hat{y} and maximizing the likelihood of the augmented data, the prediction of the response at the new location, the mean value \hat{y} , and the committed error in the prediction $\hat{\delta}^2$ are determined:

$$\hat{y}(\mathbf{x}) = \hat{\mu} + \Psi^T \Psi^{-1} (\mathbf{y} - \mathbf{1}\hat{\mu}), \quad (12)$$

$$\hat{\delta}^2(\mathbf{x}) = \hat{\sigma}^2 \left[1 - \Psi^T \Psi^{-1} \Psi + \frac{1 - \mathbf{1}^T \Psi^{-1} \Psi}{\mathbf{1}^T \Psi^{-1} \mathbf{1}} \right]. \quad (13)$$

4.1.2 Efficient Global Optimization

After the choice of the surrogate model and fitting the initial surrogate model, the optimization process starts. At this stage, the advantages of using a surrogate technique over any evolutionary algorithm can be appreciated. In fact, if not parallelized, only one call to the expensive high-fidelity model is done at each iteration. This evaluation of the true model has the role of both guiding the search towards the optimum of the optimization problem and providing new high-fidelity data (i.e., evaluations of the objective function on new infill points) to update the surrogate model and enhance its accuracy. Among other techniques for the

choice of the locations for the infill points, this work uses a modified version of Expected Improvement (EI) (Forrester et al., 2008), taking into account the connectivity constraint (Raponi et al., 2019). Since one goal of the infill search is to position the next point in order to improve the best observed value so far (y_{min}), the EI criterion aims to look for an infill position that maximizes the amount of improvement (defined as $I(\mathbf{x}) = \max(y_{min} - Y(\mathbf{x}), 0)$) over the value of the objective function measured on the current optimum:

$$\mathbf{x}_{infill} = \underset{\mathbf{x}}{\operatorname{argmax}} E[I(\mathbf{x})]. \quad (14)$$

In turn, the EI is defined as follows:

$$E[I(\mathbf{x})] = \begin{cases} (y_{min} - \hat{y}(\mathbf{x}))\Phi_Y\left(\frac{y_{min} - \hat{y}(\mathbf{x})}{\hat{s}(\mathbf{x})}\right) \\ + \hat{s}(\mathbf{x})\phi_Y\left(\frac{y_{min} - \hat{y}(\mathbf{x})}{\hat{s}(\mathbf{x})}\right) & \text{if } \hat{s}(\mathbf{x}) > 0 \\ 0 & \text{if } \hat{s}(\mathbf{x}) = 0 \end{cases} \quad (15)$$

where Φ_Y and ϕ_Y are the Gaussian cumulative distribution function and probability density function, respectively. Equation (15) can be seen as sum of two terms:

- the first term, proportional to $(y_{min} - \hat{y}(\mathbf{x}))$, which controls the exploitative tendency of the search criterion;
- the second term, proportional to $\hat{s}(\mathbf{x})$, whose predominance would lead to an explorative choice of the new infill point.

Therefore, the EI infill criterion represents a good trade off between exploitation and exploration.

4.1.3 Covariance Matrix Adaptation Evolution Strategy

The Covariance Matrix Adaptation Evolution Strategy (CMA-ES) (Hansen, 2006) is a popular algorithm for global optimization problems. The (μ, λ) -CMA-ES relies on the iterative sampling and updating of a multi-normal density

$$\vec{x}_k^{(g+1)} \sim \vec{N}\left(\langle \vec{x} \rangle_w^{(g)}, \sigma^{(g)2} \mathbf{C}^{(g)}\right), \quad k = 1, \dots, \lambda \quad (16)$$

where g is the iteration counter, $\sigma^{(g)} \in \mathbb{R}^+$ is the mutation step size, which controls the step length, and $\mathbf{C}^{(g)} \in \mathbb{R}^{n \times n}$, where n is the dimensionality of the problem, is a covariance matrix, responsible for the ellipsoidal shape of the density function. CMA-ES is a derandomized Evolution Strategy, which adapts the covariance matrix of the normal distribution on the

basis of the previous search steps (Hansen and Ostermeier, 2001). Such matrix represents pairwise dependencies between the problem variables and its update during the optimization procedure is of particular importance when dealing with ill-conditioned objective functions.

Regarding Equation (16), λ is the offspring population size and $\langle \vec{x} \rangle_w^{(g)}$ is the recombination point, which is computed as the weighted mean of selected individuals:

$$\langle \vec{x} \rangle_w^{(g)} = \sum_{i=1}^{\mu} w_i \vec{x}_{i,\lambda}^{(g)}, \quad (17)$$

with $w_i > 0$, $\forall i = 1, \dots, \mu$, and $\sum_{i=1}^{\mu} w_i = 1$. The indexing $i : \lambda$ is used to denote the i -th best individual.

The mutation parameters, i.e. the step size $\sigma^{(g)}$ and the covariance matrix $\mathbf{C}^{(g)}$, are automatically tuned by the algorithm. Such procedure happens in two steps. First of all, the global step size undergoes an adaptation process. Afterwards, $\mathbf{C}^{(g)}$ is updated according to the evolution path, the μ weighted difference vectors of the newly selected parents, and the last recombination point (Hansen, 2005).

4.1.4 Combining EGO and CMA-ES in the HKG-LSM

The main contribution of this paper is to efficiently combine CMA-ES and EGO, which are complementary techniques in the global optimization of computationally expensive functions (Mohammadi et al., 2015). EGO constructs an approximation of the high-fidelity model by evaluating the expensive objective function on a chosen training set and improves the optimum by adding new points to the model, while CMA-ES samples points according to multi-normal distribution and steadily converges towards the optimum by means of a recombination and mutation. As a consequence, it looks natural to take advantage of the potential that such methods exhibit at different stages of the optimization process. This leads to an algorithm that starts with the Designs of Experiments (DoE), which is characteristic for surrogate-based optimization techniques, and then fits an initial Kriging approximation of the high-fidelity model, getting on with the optimization of such model based on EGO. Hereafter, it switches to CMA-ES when no improvement on the objective function value is observed for a prescribed number of iterations. As already stated, such strategy is proposed in this work and referred to as Hybrid Kriging-assisted Level Set Method (HKG-LSM) for Structural Topology Optimization.

The combination of EGO and CMA-ES to obtain the HKG-LSM works as follows. If c_{max} is a pre-

determined constant value, the optimization method switches from the first to the second sub-algorithm when fitness does not improve within a budget of c_{\max} iterations. On the contrary, if the value c_{\max} has not been reached yet and the EGO finds a design with a better value of the objective function with respect to the best so far, the counter c of the iterations without any improvement on the optimum is reset to 1. The c_{\max} parameter can be chosen according to the considered problem, but, as discussed later in this work, it is convenient that the transition to CMA-ES occurs once the explorative capabilities of KG-LSM are sufficiently exploited.

At the moment of the switch between the considered sub-algorithms, the mutation step size σ of the CMA-ES optimizer is taken as the exponentially weighted average (EWA) of the differences in position between the unpromising infill points and the current optimum design during the last c_{\max} iterations of the KG-LSM, rescaled by a constant scalar α . Such EWA is iteratively computed over the $c \leq c_{\max}$ iterations as follows:

$$v_c = \begin{cases} x_{i,1}, & \text{if } c = 1 \\ \beta v_{c-1} + (1 - \beta)x_{i,c}, & \text{if } c > 1 \end{cases} \quad (18)$$

where the coefficient β represents the degree of weighting decrease, a constant smoothing factor between 0 and 1 and chosen in this work equal to 0.1 (a lower β discounts newer observations faster), $x_{i,c}$ is the value of the i^{th} component of the infill design at a time period c and v_c is the value of the EWA at any time period c . Equation (18) applies weighted factors to the positions of the infill points so that the most recent candidates have greater influence on the stepsize definition. This choice for the σ parameter is aimed to take into account the predominant tendency of the KG-LSM to explore/exploit the design space during the unsuccessful search of a new current optimum within the prescribed number of iterations c_{\max} , leading to a larger/stricter mutation step size for the Evolution Strategy as soon as the transition occurs.

4.2 Constraint Handling Techniques

During the DoE phase of the optimization algorithm, the sample points that are not feasible are automatically discarded and only feasible points are used to construct the surrogate model. Different techniques are used to deal with the connectivity and volume constraint during the infill procedure.

4.2.1 Expected Improvement for Connected Designs

The Expected Improvement for Connected Designs (EICD) is a variant of the standard EI, defined to ensure the connectivity of the promising candidates during the infill procedure (Raponi et al., 2017; Raponi et al., 2019). The main idea is to penalize the infeasible designs according to the level of infeasibility. To this end, a graph representation of the structure is used (Raponi et al., 2019). When disconnected designs are met during the maximization of EI by Differential Evolution (DE) (Storn and Price, 1997), the algorithm computes a penalty P , which takes into account the amount of violation of the connectivity constraint:

$$P = \gamma(P_1 + P_2 + P_3), \quad (19)$$

where each P_i , for $i = 1, 2, 3$, is the minimum extra-distance that has been computed according to the 1st, 2nd or 3rd type of disconnection presented in 3, and γ is a suitable penalty factor.

Such penalty is used to modify the EI criterion (15) as follows:

$$\text{EICD}(\mathbf{x}) = \begin{cases} E[I(\mathbf{x})] & \text{if } \mathbf{x} \text{ is connected,} \\ -P(\mathbf{x}) & \text{if } \mathbf{x} \text{ is disconnected,} \end{cases} \quad (20)$$

where the introduction of the penalty P is dictated by the necessity to avoid the creation of large flat areas in the landscape of the optimization problem, which might cause stagnation of the DE search.

4.2.2 Constrained Expected Improvement

In this study, the Constrained Expected Improvement (CEI) (Forrester et al., 2008) is used to generate points that satisfy a prescribed volume limit. At each iteration of the optimization strategy, an approximation of the function defining the volume constraint is also constructed. At this stage, the probability that the design satisfies the volume constraint (Probability of Feasibility (PF)) is computed as:

$$P[F(\mathbf{x})] = \frac{1}{\hat{\sigma}^2(\mathbf{x})\sqrt{2\pi}} \int_0^\infty \exp\left(-\frac{(F - \hat{g}(\mathbf{x}))^2}{2\hat{\sigma}^2(\mathbf{x})}\right) dG, \quad (21)$$

where $\hat{g}(\mathbf{x})$ is the prediction of the constraint function, $\hat{\sigma}^2(\mathbf{x})$ is the variance of the model of the constraint, and $F = G(\mathbf{x}) - V_{\text{req}}$ is the entity of feasibility. Hence, the probability that a feasible infill point improves on the best value so far can be computed by maximizing the product between EI and PF:

$$\mathbf{x}_{\text{infill}} = \underset{\mathbf{x}}{\text{argmax}} \text{CEI}(\mathbf{x}) = \underset{\mathbf{x}}{\text{argmax}} E[I(\mathbf{x})]P[F(\mathbf{x})], \quad (22)$$

where the product is justified by the independence of the models.

To consider both the connectivity and volume constraints, the coupling between EICD and CEI is obtained by applying the connectivity check in the maximization of EI·PF, leading to the following combined definition:

$$\overline{\text{EICD}}(\mathbf{x}) = \begin{cases} \text{CEI}(\mathbf{x}) & \text{if } \mathbf{x} \text{ is connected,} \\ -P(\mathbf{x}) & \text{if } \mathbf{x} \text{ is disconnected.} \end{cases} \quad (23)$$

4.2.3 Exterior Penalty Method

The techniques described in Sections 4.2.1 and 4.2.2 are appropriate for the Kriging-based EGO. Therefore, the Exterior Penalty Method (Rao, 1996) is introduced when the CMA-ES comes in. It works by penalizing the objective function values every time a constraint is not satisfied. Therefore, the objective function assumes the following shape:

$$f(\mathbf{x}) = f_{\text{obj}}(\mathbf{x}) + c \cdot \max(0, g(\mathbf{x})), \quad (24)$$

where f_{obj} is the objective function to be minimized in the original problem, g is a nonlinear constraint and c denotes a penalty constant. This leads to a modification of the objective function value that automatically rejects the penalized design. The penalty is usually taken as a very large constant value, in order to immediately ensure rejection of an infeasible design. The penalized objective function is referred to as *cost function*.

5 TEST CASE

The proposed HKG-LSM optimization strategy is here evaluated on a linear elastic test case, which is characterized by low computational costs and sufficient to draw some conclusions about the promisingness of the approach. The test is performed on the standard cantilever beam benchmark problem, whose structure is optimized to minimize compliance. The previously developed KG-LSM (Raponi et al., 2017; Raponi et al., 2019) and the EA-LSM, using CMA-ES (Hansen, 2006; Bujny et al., 2018) are taken as a reference to compare the convergence properties and the optimized designs resulting from the proposed approach.

As shown in Figure 4, the beam is fixed to a support at the left-hand side and a static unit load is applied in the middle of the right-hand side. The domain dimensions are 20×10 [mm]. The FEM mesh was generated with CalculiX, Version 2.13 (open-source, 3D structural FEM software developed at MTU Aero

Table 1: Cantilever beam test case settings.

Property	Symbol	Value	Unit
Young's modulus	E	$2.1 \cdot 10^5$	MPa
Poisson's ratio	ν	0.3	-
Load	F	1	N
Volume fraction	V_f	50 %	-
Mesh resolution	-	100 x 50	-
Element type	-	4-node shell element	-
Solver	-	CalculiX 2.9	-

Engines in Munich: <http://www.calculix.de/>). It is a structured grid composed of 5000 four-node square shell (S4R) finite elements, arranged in a 100×50 grid.

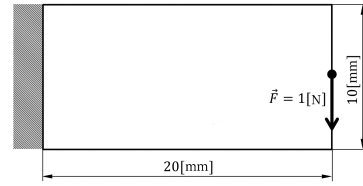


Figure 4: Problem definition of the Cantilever beam test case (Raponi et al., 2019).

If an element is located in an area of the design domain where the level-set function assumes a positive value, then it is assigned a Young's modulus equal to the one specified in the Table of Properties 1. Otherwise, only the 1% of this value is set. Therefore, at each iteration of the optimization process, throughout which the FEM mesh remains unchanged, areas corresponding to void are occupied by a very weak material.

The considered configuration consists of 6 beams symmetric with respect to a horizontal axis and evenly positioned all over the design domain (Figure 5).

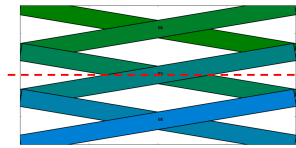


Figure 5: Reference layout of 6-beams for the static Cantilever Beam test case (Raponi et al., 2019).

This structure allows to obtain a 9 dimensional problem: for each beam, the x_0 and y_0 position parameters and the orientation θ from Equation (4) are subjected to optimization, while the length and thickness are fixed. Therefore, the vector of design variables is of the form $(x_{01}, y_{01}, \theta_1, x_{02}, y_{02}, \theta_2, x_{03}, y_{03}, \theta_3)$ and the parameters defining the remaining beams are obtained by symmetry for reducing the problem dimensionality. This test case allows to evaluate the promis-

ingness of the method and to formulate some considerations about the concurrent activity of the connectivity and volume constraints for the treated structures. As shown in Table 1, the allowed volume limit for each material distribution is set to 50% of the design domain.

6 EXPERIMENTAL EVALUATION

The following section presents the experimental setup used to test the proposed HKG-LSM and the obtained results.

6.1 Experimental Setup

The developed HKG-LSM is tested on a 6-beams 9-variables configuration. Starting from a 300-samples DoE, the following strategies are compared for a total budget of 500 calls to the objective function:

- HKG-LSM-bias10/(30/50)-exp: Hybrid Kriging-guided Level Set Method where the switch from KG-LSM to CMA-ES is done when the best observed objective value is not updated for 10/(30/50) iterations; the step size for the CMA-ES is chosen as the exponentially weighted average of the distances between the best structure and the worse infill points;
- KG-LSM: Kriging-guided optimization method with initial DoE selection by removing the infeasible points and the EICD to handle both the connectivity during the infill procedure. It is shown for comparison purposes;
- EA-LSM using CMA-ES and taking the reference structure in Figure 5 as first parent design. Here, the exterior penalty method is used to drive the search towards feasible designs. It is shown for comparison purposes.

In the KG-LSM optimization algorithm, $\theta_L = [1E-3] * 9$ and $\theta_U = [1E3] * 9$ are chosen as user-defined bounds for the theta parameter to be optimized through Maximum Likelihood Estimation, as explained in Section 4.1.1. A non-elitist (μ, λ) -CMA-ES strategy is used and initialized with a parent population of $\mu = 5$ individuals, whereas $\lambda = 10$ is the offspring population size. The mutation step is characterized by a normally distributed random vector defined by the initial mean m_{init} , while the standard deviation σ_{init} is chosen in this work as the exponentially weighted average described in Section 4.1.4.

6.2 Results

Due to the non-deterministic nature of the considered optimization algorithms, for each one 30 optimization runs are performed (with different random seeds). For each strategy, the average convergence of the compliance objective function in terms of evaluations is shown in Figure 6. Here, the objective function is normalized with respect to the reference design for the 6-beams test case defined in Section 5.

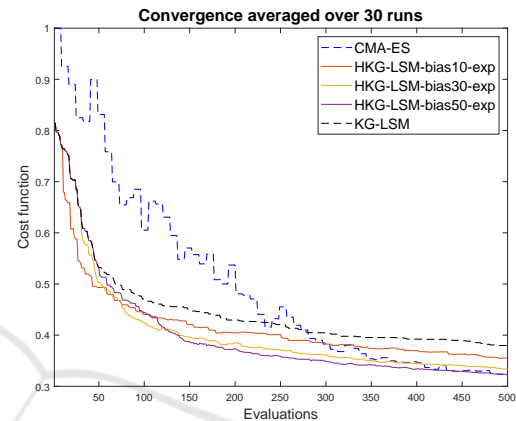


Figure 6: Convergence of the compliance function averaged over 30 runs for the HKG-LSM starting from a 300-samples DoE, with selection of feasible designs. The trends for the 10, 30 and 50-iterations bias for the switch are compared. The evaluations spent for the DoE phase are not shown in the plot since they are performed once for all the methods. The KG-LSM and the CMA-ES are also shown as a reference.

From Figure 6 it is clear that when evaluation 280 is reached, the CMA-ES seems more suitable for exploiting the best design obtained so far, leading to an unquestionably better performance over the KG-LSM. When observing the HKH-LSM strategies, the predominance of the CMA-ES is not evident anymore. In fact, the hybrid techniques take advantage of the initial rapid decrease of the objective function resulting from the Kriging-based optimization and, when no improvement is detected within a certain number of iterations, the algorithm transits to the CMA-ES. The HKG-LSM-bias50-exp provides a better convergence trend than the other hybrid techniques. Indeed, an early switch to the CMA-ES might cause an excessive exploitation of a partially optimized design, increasing its probability to converge to a local optimum. On the other hand, a late transition from KG-LSM to CMA-ES has a better chance of bringing to the Evolution Strategy a design that is the result of a more explorative strategy, which did not focus on localized areas of the problem domain, but rather found optimal designs by searching emptier ar-

eas, characterized by a high variance of the surrogate model. Such considerations can be validated by the following analysis. According to Figure 7, three main groups of material distributions, each representing a different (local) optima obtained by the HKG-LSM-bias50-exp, can be distinguished. The frequency with which they have been observed are the 20%, 20% and 40%, for the first, second and third optimum respectively. On the other hand, the same local optima could be detected after the inspection of the results obtained for the HKG-LSM-bias10-exp. Here, the percentages drop to 7%, 7% and 53%, respectively. Such data demonstrate that a premature switch to the CMA-ES might give preference to local optima, leading to a worse convergence trend for the minimization of the cost function.

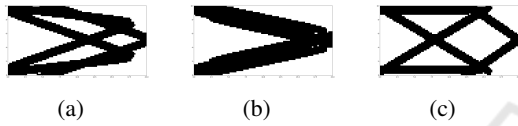


Figure 7: Three main topology types obtained with the HKG-LSM-bias50-exp method and the frequency with which they have been developed in 30 optimization runs. (a) First optimum: 20%. (b) Second optimum: 20%. (c) Third optimum: 40%.

In general, from the final structures optimized by HKG-LSM (Figure 7), it can be deduced that such methods allow sufficient flexibility for reaching designs that are not far from the theoretical one presented by Michell (Michell, 1904) for a 6-beams configuration, showed in Figure 8. In fact, at this stage, the quality of the obtained beam configurations is affected by the impossibility to vary for the length and thickness parameters of the beams. Therefore, it would be very interesting to assess the convergence capabilities of the proposed hybrid optimization techniques in higher dimensionality static and dynamic problems.

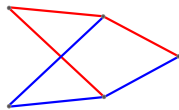


Figure 8: Michell theoretical model for a 6-beams static test case.

To conclude, further information about the optimized cost values can be found in Figure 9, which presents the statistics for each method after 100, 250 and 500 evaluations. In order to compare the medians reached by the different optimization strategies, the statistical Wilcoxon rank sum test is used. At evaluation 500, the null hypothesis that data from the different optimization methods have equal medians at the 5% significance level is accepted when

comparing HKG-LSM-bias30/50-exp with CMA-ES. This means that these strategies are comparable at the end of the considered maximum range of evaluations. Moreover, if evaluating the statistics at the beginning of the optimization process (after 100 evaluations), the same null hypothesis is rejected when comparing CMA-ES with the HKG-LSM strategies. Therefore, the HKG-LSM converges much faster than CMA-ES towards the optimum, validating the promisingness of surrogate-based strategies in case if a strict budget of evaluations is imposed.

7 CONCLUSIONS

The main aim of this work was the development of the Hybrid Kriging-assisted Level-Set Method for Topology Optimization and the evaluation of its potential and limits. The research was motivated by the need for cheap procedures in modern automotive industry, where optimization strategies demonstrated to be good alternatives to the classical trial and error method. Aimed to final applications to the crash-worthiness design optimization field, where no gradient information is available, Efficient Global Optimization (EGO) with the use of Surrogate Models - Kriging in this case - and Evolution Strategies (ESs), CMA-ES in particular, represent valid alternatives to approach the problem. Their principles are different, yet complementary: EGO constructs an approximation of the high-fidelity model by evaluating the expensive objective function on a chosen training set and improves the optimum by adding new points to the model, while CMA-ES learns and samples multi-normal laws in the space of designs variables and converges towards the optimum by means of a recombination and mutation process of the individuals. On the one hand, according to their nature, surrogate-based techniques lead to a fast convergence of the objective function towards the optimum at the beginning of the optimization procedure. On the other hand, CMA-ES steadily converges to the minimum as the number of calls to the objective function increases and has a high potential when asked to exploit some promising area of the domain, leading to a refined design with a competitive fitness if compared to its neighbors. As a consequence, it seemed natural to take advantage of the potential of such methods at different stages of the optimization process, leading to an algorithm that starts with the Designs of Experiments (DoE), fits an initial Kriging approximation of the high-fidelity model on the available data, and gets on with the optimization such model based on EGO. Finally, it switches to CMA-ES when no improvement on the best value of

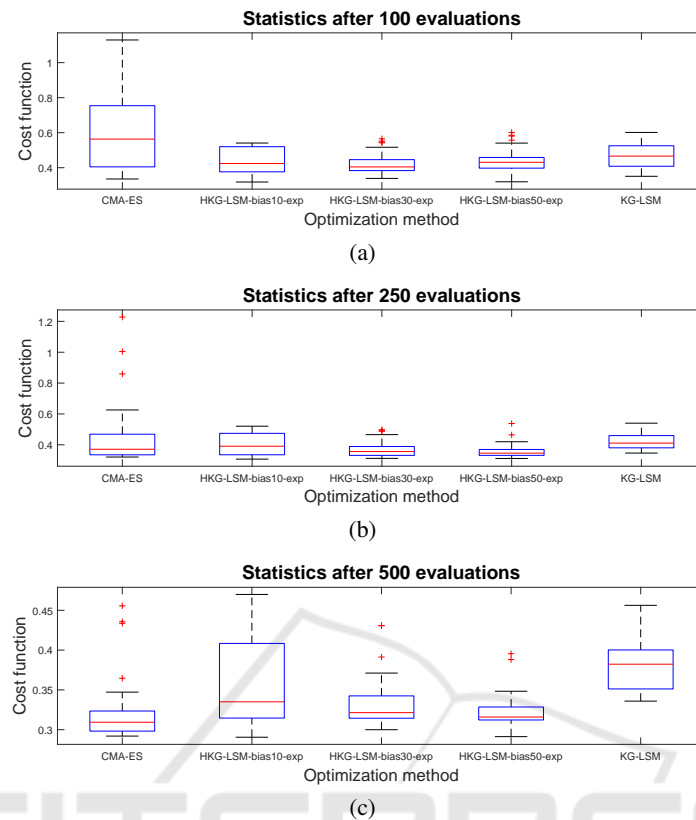


Figure 9: Statistical evaluation of the optimization methods compared for the 6-beams 9-variables cantilever beam test case: box plots for 30 runs after (a) 100, (b) 250, and (c) 500 evaluations.

the objective function is found for a prescribed number of iterations.

In this research, the potential of the proposed HKG-LSM was assessed through the study of a standard cantilever beam benchmark problem, where the objective function to be minimized was the compliance of the structure. The HKG-LSM led to significant improvements of the convergence properties in the initial stages of the optimization process, if compared to KG-LSM and EA-LSM using CMA-ES. In particular, the number of iterations preceding the transition from the first sub-algorithm to the second one proved to be relevant. The results from the static tests show that the proposed approach can be a valid alternative to both the surrogate-based and evolutionary-based methods, if taken alone, in the optimization of mechanical structures. Indeed, in the initial phase of the optimization process, significant improvements of the convergence properties could be observed, if compared with CMA-ES, while the hybrid algorithms outperform KG-LSM at the end. In view of an application to crash optimization problems, which are characterized by a limited number of available evaluations, such hybrid techniques are promising. There-

fore, further studies on static test cases of higher dimensionality and crash scenarios are planned to be done in future works. Moreover, some deeper analysis with regards to the estimation of the initial parameters for the CMA-ES is needed. In fact, the fitted Kriging mean as an approximation to the true function can be used to initialize both the covariance matrix and the step size of CMA-ES (Mohammadi et al., 2015). Lastly, new methods to combine surrogates with evolution strategies in order to obtain outperforming mechanical structures can be investigated.

REFERENCES

- Allaire, G., Jouve, F., and Toader, A. M. (2004). Structural optimization using sensitivity analysis and a level-set method. *Journal of Computational Physics*, 194(1):363–393.
- Arsenyev, I. (2017). *Efficient Surrogate-based Robust Design Optimization Method*. PhD thesis, Technische Universität München.
- Aulig, N. (2017). *Generic Topology Optimization Based on Local State Features*. PhD thesis, Technische Universität Darmstadt, VDI Verlag, Germany.

- Aulig, N. and Olhofer, M. (2016). State-based representation for structural topology optimization and application to crashworthiness. In *2016 IEEE Congress on Evolutionary Computation (CEC)*, pages 1642–1649, Vancouver, Canada.
- Bendsøe, M. P. and Sigmund, O. (2004). *Topology Optimization - Theory, Methods, and Applications*. Springer Berlin Heidelberg, second edition.
- Bujny, M., Aulig, N., Olhofer, M., and Duddeck, F. (2016). Evolutionary Level Set Method for Crashworthiness Topology Optimization. In *VII European Congress on Computational Methods in Applied Sciences and Engineering*, Crete Island, Greece.
- Bujny, M., Aulig, N., Olhofer, M., and Duddeck, F. (2018). Identification of optimal topologies for crashworthiness with the evolutionary level set method. *International Journal of Crashworthiness*, 23(4):395–416.
- Cressie, N. (1990). The origins of kriging. *Mathematical Geology*, 22(3):239–252.
- Duddeck, F., Hunkeler, S., Lozano, P., Wehrle, E., and Zeng, D. (2016). Topology optimization for crashworthiness of thin-walled structures under axial impact using hybrid cellular automata. *Structural and Multidisciplinary Optimization*, 54(3):415–428.
- Duddeck, F. and Volz, K. (2012). A new Topology Optimization Approach for Crashworthiness of Passenger Vehicles Based on Physically Defined Equivalent Static Loads. In *ICrash International Crashworthiness Conference*, Milano, Italy.
- Eschenauer, H. A., Kobelev, V. V., and Schumacher, A. (1994). Bubble method for topology and shape optimization of structures. *Structural optimization*, 8(1):42–51.
- Fang, K. T., Li, R., and Sudjianto, A. (2005). *Design and Modeling for Computer Experiments*. CRC Press.
- Forrester, A. I. J., Sobester, A., and Keane, A. J. (2008). *Engineering Design via Surrogate Modelling - A Practical Guide*. John Wiley & Sons Ltd.
- Guo, X., Zhang, W., and Zhong, W. (2014). Doing Topology Optimization Explicitly and Geometrically - A New Moving Morphable Components Based Framework. *Journal of Applied Mechanics*, 81(8):081009.
- Haber, R. and Bendsøe, M. P. (1998). Problem Formulation, Solution Procedures and Geometric Modeling: Key issues in Variable-Topology Optimization. In *7th AIAA/USAF/NASA/ISSMO Symposium on Multidisciplinary Analysis and Optimization*, St. Louis, Missouri, USA.
- Hansen, N. (2005). The CMA Evolution Strategy: A Tutorial. hal-01297037f.
- Hansen, N. (2006). The CMA Evolution Strategy: A Comparing Review. In *Towards a New Evolutionary Computation*, Studies in Fuzziness and Soft Computing, pages 75–102. Springer Berlin Heidelberg. DOI: 10.1007/3-540-32494-1_4.
- Hansen, N. and Ostermeier, A. (1996). Adapting arbitrary normal mutation distributions in evolution strategies: the covariance matrix adaptation. In *Proceedings of IEEE International Conference on Evolutionary Computation*, pages 312–317.
- Hansen, N. and Ostermeier, A. (2001). Completely Derandomized Self-Adaptation in Evolution Strategies. *Evolutionary Computation*, 9(2):159–195.
- Jones, D. R., Schonlau, M., and Welch, W. J. (1998). Efficient Global Optimization of Expensive Black-Box Functions. *Journal of Global Optimization*, 13(4):455–492.
- Kleijnen, J. P. C. (2009). Kriging metamodeling in simulation: A review. *European Journal of Operational Research*, 192(3):707–716.
- Lee, H.-A. and Park, G.-J. (2015). Nonlinear dynamic response topology optimization using the equivalent static loads method. *Computer Methods in Applied Mechanics and Engineering*, 283:956–970.
- Michell, A. G. M. (1904). LVIII. The limits of economy of material in frame-structures. *Philosophical Magazine*, 8(47):589–597.
- Mohammadi, H., Riche, R. L., and Touboul, E. (2015). Making EGO and CMA-ES Complementary for Global Optimization. In *Learning and Intelligent Optimization*, Lecture Notes in Computer Science, pages 287–292. Springer, Cham.
- Mozumder, C., Renaud, J. E., and Tovar, A. (2012). Topometry optimisation for crashworthiness design using hybrid cellular automata. *International Journal of Vehicle Design*, 60(1-2).
- Ortmann, C. and Schumacher, A. (2013). Graph and Heuristic Based Topology Optimization of Crash Loaded Structures. *Structural and Multidisciplinary Optimization*, 47(6):839–854.
- Osher, S. and Sethian, J. A. (1988). Fronts propagating with curvature-dependent speed: Algorithms based on Hamilton-Jacobi formulations. *Journal of Computational Physics*, 79(1):12–49.
- Pedersen, C. B. W. (2003). Topology optimization design of crushed 2d-frames for desired energy absorption history. *Structural and Multidisciplinary Optimization*, 25(5-6):368–382.
- Rao, S. S. (1996). *Engineering Optimization: Theory and Practice*. John Wiley & Sons.
- Raponi, E., Bujny, M., Olhofer, M., Aulig, N., Boria, S., and Duddeck, F. (2017). Kriging-guided Level Set Method for Crash Topology Optimization. In *7th GACM Colloquium on Computational Mechanics for Young Scientists from Academia and Industry*, Stuttgart, Germany.
- Raponi, E., Bujny, M., Olhofer, M., Aulig, N., Boria, S., and Duddeck, F. (2019). Kriging-assisted topology optimization of crash structures. *Computer Methods in Applied Mechanics and Engineering*, 348:730–752.
- Storn, R. and Price, K. (1997). Differential Evolution – A Simple and Efficient Heuristic for global Optimization over Continuous Spaces. *Journal of Global Optimization*, 11(4):341–359.